Autophagic degradation of CDK2 and CDK4 is responsible for NVP-BEZ235-induced G0/G1 cell cycle arrest in neuroblastoma

Zhen Liu
Shanghai 9th Peoples Hospital Affiliated to Shanghai Jiaotong University School of Medicine
Hong–Liang Zhang
Central China Fuwai Hospital of Zhengzhou University
Shan-Ling Liu
Shanghai 9th Peoples Hospital Affiliated to Shanghai Jiaotong University School of Medicine
Chao Zhang
Shanghai 9th Peoples Hospital Affiliated to Shanghai Jiaotong University School of Medicine
Qing-Xi Yue
Shanghai 9th Peoples Hospital Affiliated to Shanghai Jiaotong University School of Medicine
Quan-Wu Zhang
Zhengzhou Central Hospital Affiliated to Zhengzhou University
Feng-Hou Gao (631484@2m9h.net)
Shanghai Jiao Tong University School of Medicine

Research article

Keywords: CDK2, CDK4, NVP-BEZ235, Autophagic degradation, Cell cycle

Posted Date: May 18th, 2021

DOI: https://doi.org/10.21203/rs.3.rs-531206/v1

Abstract

Background

Cyclin-dependent kinases (CDKs) are regarded as promising targets for cancer therapy. CDK2 and CDK4 are the core molecules in the G0 and G1 phases of the cell cycle. Exploring the molecular mechanism of CDK2 and CDK4 protein degradation will provide clues and solutions to control the G0 and G1 phases in tumor cells.

Methods

The expression levels of CDK2 and CDK4 were assessed by Western blotting and qRT-PCR. Cell viability, cell proliferation and growth were evaluated in CCK-8 and flow cytometric analysis. Protein interactions were analysed by immunoprecipitation and immunofluorescence methods.

Results

NVP-BEZ235 induced neuroblastoma cell arrest at the G0/G1 phase, and proliferation inhibition was associated with a significant reduction in the CDK2 and CDK4 proteins in a dose-dependent manner at nanomolar concentrations. Surprisingly, we found that the NVP-BEZ235-induced downregulation of CDK2 and CDK4 was dramatically rescued by autophagy-lysosome inhibitors. Additionally, the blockade of autophagy-related genes contributed to the remarkable rescue of CDK2 and CDK4, which thus strikingly improved NVP-BEZ235-induced G0/G1 arrest and growth inhibition of neuroblastoma cells. Subsequently, we observed the first evidence that NVP-BEZ235 induced the interaction of p62/SQSMT1 with CDK2 or CDK4 and the autophagic degradation of CDK2 and CDK4 in a cathepsin B-dependent manner. Analogous results regarding autophagy and the antiproliferative effects of NVP-BEZ235 were observed in a neuroblastoma xenograft mouse model in vivo.

Conclusions

These results not only established the pivotal role of the autophagy pathway in G0/G1 cell cycle-related protein turnover but also suggest the potential application of NVP-BEZ235 for cancer treatment by modulating elements of the autophagic machinery to promote degradation of G0/G1 cell cycle-related proteins.

Background

The cell cycle process is orchestrated by the interplay of various cyclin/CDK combinations and other key cell cycle-related proteins at checkpoints to ensure unidirectional and irreversible cell division in eukaryotes[1–3]. As a critical regulator of cell proliferation, deregulation of the cell cycle universally leads

to the development and progression of human cancers[4, 5]. Hence, targeting cell cycle control, especially aiming at disrupting the related signaling pathways, may become a promising therapeutic approach. Activation of the PI3K-Akt-mTOR pathway has recently attracted considerable attention due to its correlation with abnormalities of cell cycle regulation and tumor growth, and several targets of the PI3K-Akt-mTOR pathway are interrelated with cell cycle progression, including MDM2, GSK3β, p70S6K, and 4EBP1[6, 7]. These results suggest that inhibitors of this pathway may be a useful avenue for therapeutic intervention in cancer patients.

NVP-BEZ235 is a synthetic small molecule compound that potently and reversibly inhibits the catalytic activities of PI3K and mTOR by competing at their ATP-binding sites[8]. As a dual PI3K/mTOR inhibitor, NVP-BEZ235 shows the potential characteristics of overcoming resistance, which was observed in the negative feedback loop activation of Akt due to mTORC1 inhibitors, such as rapamycin[9], and activation of MAPK signaling with PI3K inhibitors, such as LY294002[10]. NVP-BEZ235 is the most effective small molecule inhibitor of PI3K to date and has been a particularly attractive compound with the traits of a low dose requirement, good tolerance, a notable effect and greater selectivity compared with other dual inhibitors. Multiple studies have demonstrated the prominent inhibitory efficacy of NVP-BEZ235 on the proliferation in a wide variety of human malignant tumors in vitro and preclinical animal models and are currently in phase I/II clinical trials for advanced solid tumors[11, 12]. It is generally believed that cell cycle arrest triggered by NVP-BEZ235 by antagonizing the PI3K/mTOR signaling pathway plays a pivotal role in its potent cytostatic effects. Previous observations have revealed that NVP-BEZ235 blocks the cell cycle at the G0/G1 phase, ultimately causing the interruption of cancer growth with the down regulation of cyclic D1 and pRb and the upregulation of p21 and p27 in multiple cancers, including neuroblastoma (NB)[13], osteosarcoma[14], B cell lymphoma[15] and nasopharyngeal carcinomas[16]. Additionally, it has been reported that NVP-BEZ235 can enhance the radiosensitivity of resistant prostate and glioblastoma cells through the attenuation of DNA double-strand break (DSB) repair and implementation of G2/M cell cycle arrest[17, 18]. However, the precise mechanisms by which NVP-BEZ235 influences cell cycle distribution via down regulation of cell cycle-related proteins remain largely unknown.

In the current research, NB models with excessive activation of the PI3K/Akt/mTOR pathway were used to evaluate the effect of NVP-BEZ235 on cell cycle arrest and investigate the concrete mechanisms by which NVP-BEZ235 induces the down regulation of cell cycle-related proteins. Our results indicated that NVP-BEZ235 facilitated autophagic degradation of CDK2 and CDK4, which can rapidly induce NB cell cycle arrest at G0/G1 state and proliferation inhibition.

Methods

Reagent, cell lines and cell culture

NVP-BEZ235 was purchased from Novartis (Selleck, S1009) and dissolved in DMSO to a stock concentration of 1 mmol/L. CQ (Sigma-Aldrich, C6628), and 3-MA (Sigma-Aldrich, M9281) were obtained and dissolved in sterile H_2O to stock concentrations of 20 mmol/L and 100 mmol/L, respectively. CHX

was purchased from Sigma (Sigma-Aldrich, R750107) and dissolved in ethanol at a stock concentration of 100 mg/ml. The stock solutions were wrapping in foil and maintained at -20°C.

SH-SY5Y and SK-N-MC cell lines were obtained from the Shanghai Institutes for Biological Sciences (Shanghai, China) and were cultured in RPMI 1640 medium containing 10% fetal bovine serum (FBS) (Gemini, 100-700) and 1% penicillin-streptomycin (Gibco, 15140122) under standard culture conditions (37°C and 5% CO_2). Cells in the logarithmic phase of growth were used in all experiments.

Cell Counting Kit-8 assay

Cell proliferation was assessed using the Cell Counting Kit-8 reagent (Dojindo Molecular Technologies, CK04). SH-SY5Y and SK-N-MC cells were seeded in 96-well culture plates at 5×10^3 cells/well in triplicate, allowed to settle overnight, and treated with serial concentrations of NVP-BEZ235 (0, 100 and 200 nmol/l) in 200 µl of medium for 24 hours. Transfected cells were treated with 200 nmol/l NVP-BEZ235 or DMSO for 12 hours. The cells were then treated with CCK-8 solution and incubated for 2 hours according to the CCK-8 kit instructions. The absorbance was measured at 450 nm using a microplate reader (Bio-Rad, Hercules, CA, USA). Each experiment was performed at least 3 times independently.

Cell cycle by flow cytometric analysis

NB cells in exponential growth were seeded in 6-well plates at a density of 1×10^6 per well for 24 hours attachment, after which they were treated with NVP-BEZ235 (0, 100 and 200 nM) for 24 hours, and the transfected cells were treated with 100 nM NVP-BEZ235 or DMSO for 12 hours. For cell cycle analysis, cells were digested with 0.25% trypsin, centrifuged at 2000 ×g for 5 minutes, washed three times with PBS and fixed with ice-cold 75% (v/v) ethanol at -20°C for 2 hours. Then, after washing twice with PBS, the cells were resuspended in 50 µl of PI solution (PI 50 µg/ml and RNase A 100 µg/ml). After incubation for 15 minutes at room temperature in the dark, the cell cycle distribution was analyzed by a FACSCanto flow cytometer (Becton Dickinson, Franklin Lakes, NJ, USA).

Western blot analysis

Cultured cells or mouse tumor tissues were homogenized on ice in 1× RIPA lysis buffer containing phosphatase (Roche, 4906845001) and protease inhibitor cocktail (Roche, 4693116001), and the protein concentration was measured by a BCA Protein Assay Kit (Takara, T9300A). Equal amounts (50 µg) of isolated proteins were separated by SDS polyacrylamide gel electrophoresis and transferred to PVDF membranes. Membranes were blocked in 5% nonfat milk in Tris-buffered saline containing 0.1% Tween-20 (TBST, pH 7.4) for 1 h at room temperature and incubated overnight at 4°C at a dilution of 1:1000 with primary antibodies against Pi-RB, CDK2, CDK4, GAPDH, CTSB, CTSD, p62, LC3B and Beclin-1 (all from Cell Signaling Technology). Then, the membranes were probed for 2 hours at room temperature with species-specific HRP-conjugated rabbit anti-mouse IgG (Cell Signaling Technology) at a dilution of 1:10000. Immunoreactive bands were identified with the Immobilon Western Chemiluminescent HRP Substrate (Millipore Co., 1328701).

Immunoprecipitation assays

After washing in cold PBS, cells or tissues were lysed in 500 μl of ice-cold RIPA lysis buffer (50 mM Tris-HCl pH 7.4, 1 mM EDTA, 0.5% sodium deoxycholate, 1% NP-40, 0.1% SDS, and 150 mM NaCl) containing protease and phosphatase inhibitors on ice for 30 minutes. Total cell lysates were clarified by centrifugation at 12,000 ×g for 15 minutes at 4°C and were divided into two parts, with one (400 μl, 500 μg) used for the immunoprecipitation assays and the other (50 μl) used for total protein analysis. Lysate supernatants were incubated with 3 μg of anti-p62 antibody or rabbit IgG overnight at 4°C with rotation, followed by preclearing with a 50% protein A/G agarose slurry for 2 hours, and then the complexes were incubated with protein A/G agarose for 4 hours at 4°C. After washing 5 times with lysis buffer by centrifugation at 5,000 rpm for 5 minutes, samples were eluted in 2X SDS loading buffer by boiling for 8 min and subjected to immunoblot analysis with anti-CDK2, anti-CDK4 or anti-ubiquitin antibodies.

Immunofluorescence assays

NB cells were cultivated in a 96-well plate exposed to various concentrations (0, 200 nM) of NVP-BEZ235 for 24 hours. After washing twice with PBS, the cells were fixed with 4% paraformaldehyde/PBS for 15 min at room temperature. Cells were then washed three times with cold PBS, permeabilized with methyl alcohol for 10 min, and finally washed with 0.05% Tween-20/PBS for 5 min. The cells were blocked with 5% BSA/PBS (Sangon Biotech, A0332) for 2 hours at room temperature and then incubated with primary antibodies (1:100) overnight at 4°C. After washing three times with 0.05% Tween/PBS, the cells were incubated with a FITC-conjugated secondary antibody (ZF-0312, 1:100) for 2 hours at room temperature in a dark humid chamber. The cell nuclei were stained with DAPI (Sigma-Aldrich, D9542). The cells were visualized by a fluorescence microscope (Nikon Eclipse Ti, Japan).

Quantitative real-time RT-PCR (qRT-PCR)

Total cellular RNA was extracted from NB cell lines using TRIzol. The reaction was performed in Micro Amp Optical 96-well plates with SYBR Premix ExTaq™ II (Takara, RR820Q) in a Real-Time PCR Detection System (Roche, Basel, Switzerland) according to the manufacturer's instructions. Related gene expression was assessed after normalization to the housekeeping gene human β-actin. Primers were designed and synthesized by Sangon Biotech Co., Ltd. (Shanghai, China). The sequences of the primers used are as follows: CDK2 primer (forward (5´-GTACCTCCCCTGGATGAAGAT-3´) and reverse (5´-CG AA AT CC GC TTGTTAGGGTC-3´)); CDK4 primer (forward (5´-CTGGTGTTTGAGCATGTAGA CC-3´) and reverse (5´-GATCCTTGATCGTTTCGGCTG-3´)).

Lentiviral transduction

The shRNA pGIPZ lentiviral constructs were obtained from Hanbio (Shanghai, China). The sequences used are as follows: a. Beclin-1 #1 (5'-CCC GTG GAA TGG AAT GAG ATT-3'), Beclin-1 #2 (5'-GCT TGG GTG TCC TCA CAA TTT-3'); b. ATG7#1 (ACC AGT TCA GAG CTA A), ATG7#2 (ACC AGT TCA GAG CTA AAT A); c. Scrambled (5'-GTG GAC TCT TGA AAG TAC TAT-3'). The pGIPZ vectors and packaging plasmids

(psPAX2, pMD2.G) (Life Technologies, Carlsbad, CA, USA) were cotransfected into packaging 293T cells using Lipofectamine-3000 (Life Technologies, L3000001). After 48 hours, the viral supernatants were collected and used to infect SH-SY5Y cells. Stable clones expressing the shRNAs were obtained via 5 μg/ml puromycin dihydrochloride (Santa Cruz Biotech Inc., sc-205821) selection.

RNA interference

Small interfering RNAs (siRNAs) specific to human CTSB, CTSD and negative control siRNA were synthesized by GenePharma (Shanghai, China). The sequences used are as follows: CTSB (5'-UGG UCA ACU AUG UCA ACA ATT-3'); CTSD (5'-UCA CCU UCA UCG CAG CCA ATT-3'); p62 (5'-GAA UCU ACA UUA AAG AGA ATT-3'); negative control (5'-UUC UCC GAA CGU GUC ACG UTT-3'). Both cell lines were transfected with siRNA using Lipofectamine-3000 (Life Technologies) according to the manufacturer's protocol.

Nude mouse xenograft model of NB cancer

Animal experiments were approved by the Institutional Animal Care and Use Committee (IACUC) of Shanghai Jiao Tong University. Five- to six-week-old female athymic (nu/nu) mice were housed under pathogen-free conditions in microisolator cages with laboratory chow and water ad libitum. SH-SY5Y cells (5×10^6) suspended in 100 μl of PBS were injected s.c. into the flank region of nude mice. When the size of local tumors reached certain ranges (~50 mm^3), the mice were randomized into two groups according to tumor volumes and body weights for the following treatments: vehicle control (DMSO) and NVP-BEZ235 (20 mg/kg/day, i.p.). Mice were euthanized after 3 weeks of interventions, and tumor tissues were excised[19].

Statistical analysis

In all figures, the error bars represent the standard deviations. Statistical analyses were performed by Microsoft Office Excel 2019 (Microsoft, Albuquerque, NM, USA) and Statistica Version 10.0 (StatSoft, Tulsa, OK, USA). Differences between mean values were evaluated by the unpaired t-test. Differences were considered statistically significant at $P<0.05$.

Results

NVP-BEZ235 could induce G0/G1 cell cycle arrest with the down regulation of the CDK 2 and CDK 4 proteins.

We analyzed the effect of NVP-BEZ235 on cell cycle progression in NB cells by flow cytometry using PI staining of the DNA content. After exposure to 100 nM and 200 nM NVP-BEZ235 for 24 hours, there was a significant increase in the percentage of the SH-SY5Y cells in the G0/G1 phase (82.28%±2.86% at 100 nM, 85.98%±1.93% at 200 nM) compared with the control group (66.82%±3.50%) (Fig. 1A). A significant increase in G0/G1 phase cells was also detected in SK-N-MC cells (Fig. 1B). To further investigate the correlation of NVP-BEZ235-induced G1 cell cycle arrest with some important G1-phase regulatory proteins

in NB cells. The expression of endogenous CDKs was assessed when SH-SY5Y and SK-N-MC cells were treated with 200 nM NVP-BEZ235 for various times. CDK4 and CDK2 are significant G1 phase-associated regulatory proteins governing the restriction point of G1→S phase progression, and their inhibition or degradation lead to G1 phase arrest[20]. As indicated in Fig. 1C and D, there was a remarkable reduction or gradual decrease in CDK4 and CDK2 protein levels in both cell lines. Furthermore, phospho-Rb initially triggered by dependent kinases and then amplified by CDK2 complexes markedly decreased in a time-dependent manner. This process is critical for the G1- to S-phase transition, as phospho-Rb results in the release of active E2F, which stimulates the transcription of the gene-mediated G1 phase. Based on the above results, we concluded that NVP-BEZ235 exerts notable G0/G1 cell cycle arrest in NB cells through the down regulation of several key G1-phase regulatory proteins.

NVP-BEZ235 attenuated the G0/G1 cell cycle-related protein levels by facilitating their protein degradation.

To elucidate whether NVP-BEZ235-mediated down regulation of CDK4 and CDK2 proteins results from transcriptional or posttranscriptional regulation, their mRNA levels were evaluated by qRT-PCR. As shown in Fig. 2A and B, the mRNA levels of CDK4 and CDK2 were not drastically altered in the presence of 200 nM NVP-BEZ235. This indicates that NVP-BEZ235 may affect the protein stability of CDK4 and CDK2 that were detected via CHX-chase analysis. As showed in Fig. 2C-H, NB cells were cotreated with 10 μg/ml CHX for different time followed by pretreatment with 200 nM NVP-BEZ235 for 1 hour. NVP-BEZ235 obviously attenuated the half-life of these proteins in both cell lines. These data suggested that NVP-BEZ235 reduces CDK4 and CDK2 protein stability and promotes their degradation.

Autophagy-lysosome inhibitors restored the degradation of CDK2 and CDK4 proteins in NVP-BEZ235-treated NB cells.

To clarify whether the ubiquitin-proteasome pathway is involved in the degradation of CDK2 and CDK4 proteins, we pretreated SH-SY5Y and SK-N-MC cells with the 26S proteasome inhibitor MG132 (10 μM) for 1 hour, followed by treatment with 200 nM NVP-BEZ235 for 12 hours. Compared with the NVP-BEZ235 single factor treatment group, the CDK2 and CDK4 proteins in the MG132 and NVP-BEZ235 dual factor treatment groups did not change significantly (Fig. 3A and B). In addition to the effect on cell proliferation, the PI3K/Akt/mTOR pathway is also involved in the autophagy process. We further assessed autophagy-related hallmark proteins in both cell lines treated with NVP-BEZ235. As showed in Fig. 3C and D, NVP-BEZ235 enhanced the conversion of LC3-II in both tested cell lines at an early stage. Given that the activation of autophagy almost exactly synchronized with the down regulation of CDK4 and CDK2 proteins, we speculated that autophagy induced by NVP-BEZ235 might play a role in cell cycle arrest. To prove our hypothesis, the effects of the autophagy inhibitors CQ and 3-MA were analyzed. Intriguingly, cotreatment with CQ or 3-MA for 12 hours rescued the expression of CDK2 and CDK4 (Fig. 3E-H).

NVP-BEZ235-induced G0/G1 cell cycle arrest and proliferation inhibition by autophagy activation in NB cells.

Autophagy is one of the two major key intracellular protein degradation routes within eukaryotic cells[21]. To further verify whether NVP-BEZ235-induced autophagy influences NB cells, we tested the effect of inhibition of the autophagic process on CDK4 and CDK2 degradation, cell viability and cell cycle distribution via knockdown of autophagy-related genes. Accordingly, SK-N-MC cells that were transfected with shRNA for the knockdown of Beclin-1 were subsequently treated for 12 hours with vehicle or 200 nM NVP-BEZ235. CDK4 and CDK2 were analyzed by immunoblotting, cell viability was assessed using a CCK-8 assay, and cell cycle distribution was demonstrated with flow cytometry analysis. We found that blockade of autophagy (Fig. 4A) markedly reversed the CDK2 and CDK4 protein levels (Fig. 4B). Simultaneously, the viability of NVP-BEZ235-treated NB cells was obviously rescued (Fig. 4C), and the percentage of NVP-BEZ235-treated cells in the G0/G1 phase was strikingly increased (Fig. 4D) due to autophagy inhibition. These results demonstrated that the autophagy-mediated degradation pathway plays roles in NVP-BEZ235-induced G0/G1 cell cycle arrest and proliferation inhibition in NB cells.

NVP-BEZ235-induced CDK2 and CDK4 binding to the autophagy adaptor protein p62 in NB cells.

P62 (known as SQSTM1) is implicated in autophagic cargo recognition and is degraded in the final stages of autophagy during autolysosome degradation[22]. A time-dependent reduction in p62 expression was corroborated in both NB cell lines treated with NVP-BEZ235 (Fig. 5A and B), consistent with the upregulation of LC3 II levels (Fig. 3C and D). To further validate the link between p62 and the CDK2 and CDK4 proteins, the levels of the p62 protein were measured in ATG7-deleted SH-SY5Y cells and Beclin-1-deleted SK-N-MC cells after treatment with 200 nM NVP-BEZ235 for 12 hours. As showed in Fig. 5C and D, there was concomitant restoration of p62 in NVP-BEZ235-treated autophagy-defective cells compared with the negative control. Moreover, immunoprecipitation assays indicated that the interactions between p62 and the CDK2 and CDK4 proteins were enhanced after exposure to NVP-BEZ235 in NB cells (Fig. 5E and F). On this basis, the degradation of the CDK2 and CDK4 proteins induced by NVP-BEZ235 was restored when p62 was silenced in NB cells (Fig. 5G and H). These findings indicated that p62 is involved in autophagic degradation of the CDK2 and CDK4 proteins in NB cells.

Lysosomal cathepsin B was indispensable for autophagic degradation of the CDK2 and CDK4 proteins induced by NVP-BEZ235.

To further substantiate CDK2 and CDK4 protein degradation due to autophagic lysosomes, we performed immunofluorescence staining for CDK2 and CDK4 and the lysosomal membrane marker LAMP2A in SH-SY5Y cells and observed a strong colocalization between them after NVP-BEZ235 treatment (Fig. 6A and B). Lysosomal cathepsins have been implicated in autophagic flux facilitation and in mediating substrate protein degradation[23] in the final stage of autophagy. To validate the functional role of cathepsins in the degradation of CDK2 and CDK4 induced by NVP-BEZ235, lysosomal-specific protease inhibitors E64d and pepstatin A were administered to SH-SY5Y cells. Importantly, suppression of cathepsins stabilized the CDK2 and CDK4 protein levels and reversed NVP-BEZ235-mediated degradation of CDK2 and CDK4 proteins (Fig. 6C). Herein, we mainly focused on the regulatory effects of cathepsin B (CTSB) and cathepsin D (CTSD) on CDK2 and CDK4 degradation. We observed that silencing CTSD expression by

utilizing a siRNA approach did not rescue CDK2 and CDK4 degradation (Fig. 6D), whereas attenuation of CTSB by siRNA targeting resulted in a partial rescue of the NVP-BEZ235-induced CDK2 and CDK4 down regulation in SH-SY5Y cells (Fig. 6E). Altogether, these results indicated that CDK2 and CDK4 enter lysosomes and undergo degradation in a CTSB-dependent manner.

Autophagy-lysosome system mediates NVP-BEZ235-triggered CDK2 and CDK4 degradation in NB xenograft tumors.

To determine the association of its autophagy with CDK2 and CDK4 protein degradation, an NB xenograft mouse model was generated. In agreement with the blockade of the G1 cell cycle in vitro, NVP-BEZ235 also reduced the expression of CDK2 and CDK4 in xenograft tumors, accompanied by a decrease in the autophagic protein marker p62 (Fig. 7A). Furthermore, the enhanced interactions between p62 and the CDK2 and CDK4 proteins were similarly assessed by immunoprecipitation in the NVP-BEZ235-treated group (Fig. 7B), which demonstrated that the autophagy-lysosome system mediates NVP-BEZ235-triggered CDK2 and CDK4 degradation. Together, these results revealed that NVP-BEZ235-induced autophagy plays a critical role in CDK2 and CDK4 degradation and tumor proliferation inhibition in NB xenografts.

Discussion

The PI3K/Akt/mTOR signaling pathway is vital in maintaining cell growth, proliferation, and survival[24]. NVP-BEZ235, as a potent novel dual PI3K and mTOR kinase inhibitor, exerts strong anticancer effects via multiple mechanisms, including disturbing the cell cycle and differentiation and promoting apoptosis, autophagy, angiogenesis and EMT[17, 25, 26]. In the present study, we demonstrated that NVP-BEZ235 inhibited NB cell proliferation by inducing G0/G1 cell cycle arrest and that inducing G0/G1 cell cycle arrest was correlated with autophagic degradation of the CDK2 and CDK4 proteins.

We have shown that there was a remarkable reduction or gradual decrease in cyclin D1 and E1 protein levels in NVP-BEZ235-treated NB cells[19]. Previous evidence that the overexpression of cyclin D1, cyclin E1, CDK2 and CDK4 has been associated with poor prognosis and decreased survival in patients, and deregulated degradation appears to be responsible for their increased levels in various cancers[27–29]. Therefore, our results are significant and suggest that NVP-BEZ235 triggered a decrease in these proteins. Given the significance of these G1 phase-related proteins, we then probed the mechanism of NVP-BEZ235-mediated down regulation of CDK2 and CDK4 in NB. The results indicated that NVP-BEZ235 did not obviously change the mRNA levels but obviously attenuated the half-life of these proteins and promoted their degradation, as confirmed by the CHX-chase analysis.

In our work, we identified for the first time that the autophagic process induced by NVP-BEZ235 is involved in the degradation of CDK2 and CDK4 in NB cells, as there is evidence that ablating autophagy-related genes and autophagy-lysosomal inhibitors could obviously reverse CDK2 and CDK4 in NVP-BEZ235-incubated NB cells. With regard to CDK2 and CDK4, there are several potential molecular weight compounds that could influence their regulation, mainly through elimination of CDK catalytic activity and

induction of their degradation[30–33]. Disappointing results were observed in CDK inhibitors in terms of low specificity, serious side effect profiles and a lack of robust criteria for selecting patients[34]. Thus, targeting compounds to induce CDK-sustained degradation is inspiring and imperative. Our studies provide evidence for a novel mechanism involving autophagic degradation of CDK2 and CDK4, which is distinct from previous reports on the degradation of CDK2 and CDK4[32, 33, 35, 36].

Our subsequent experiments elaborate the particular modulatory mechanism of autophagy in NVP-BEZ235-induced CDK2 and CDK4 degradation. Autophagy is an evolutionarily conserved pathway that delivers substrates to lysosomes for degradation. P62/SQSTM1, as a cargo receptor protein, can bind directly to LC3 to promote the degradation of polyubiquitinated protein targets via macro-autophagy[37]. Obviously, p62 is required for constitutive autophagic degradation of CDK2 and CDK4, as illustrated in our results in which an enhanced interaction between p62 and the CDK2 and CDK4 proteins was observed and the degradation of CDK2 and CDK4 induced by NVP-BEZ235 was restored when p62 was silenced in NB cells. Analogous results regarding the correlation of p62 and the CDK2 and CDK4 proteins were observed in an NB xenograft mouse model in vivo. Moreover, intensive studies have shown that CTSB, as a notable lysosomal protease, is broadly up regulated in cancer and is essential for autophagic flux[38, 39]. Our data also implicated CDK2 and CDK4 as downstream substrates of CTSB in the autophagy process, as supported by our experiments in which selective knockdown of CTSB resulted in the partial reversal of CDK2 and CDK4 degradation. Based on these findings, we demonstrate that NVP-BEZ235 induces CDK2 and CDK4 binding to the autophagy adaptor protein p62 at the autophagosome site to enter the autolysosome, which are then degraded in a CTSB-dependent manner.

Conclusion

Taken together, these results clearly indicated that NVP-BEZ235 can mediate the autophagic degradation of CDK2 and CDK4 in a CTSB/p62-dependent manner. These events preserve the cells in G0/G1 status and alleviate growth. Therefore, NVP-BEZ235 can exhibit a strong anti-proliferation effect in NB cells (Fig. 7C). This finding provides the experimental basis that NVP-BEZ235 intervenes in the regulation of CDK2 and CDK4 at the posttranscriptional level. At the same time, these findings also provide a new clue for the rational utilization of NVP-BEZ235 in neuroblastoma.

Abbreviations

NB neuroblastoma

CDK2 cyclin dependent kinase 2

CDK4 cyclin dependent kinase 4

CTSB cathepsin B

CTSD cathepsin D

PI3K phosphatidyl inositol 3-kinase

Akt v-akt murine thymoma viral oncogene homolog

mTOR mammalian target of rapamycin

MCM2 mini-chromosome maintenance protein 2

MDM2 murine double minute 2

3-MA 3-methyladenine

CQ chloroquine

ATG7 autophagy-related gene 7

CHX cycloheximide

LC3 microtubule-associated protein light chain 3

SQSTM1 sequestosome 1

siRNA small interfering RNA

E2F the e2 factor

shRNA short hairpin RNA

EMT epithelial-mesenchymal transition.

Declarations

Ethics approval and consent to participate

We used NB cell lines SH-SY5Y and SK-N-MC, which were intended for research use only, from the Shanghai Institutes for Biological Sciences (Shanghai, China). Animal experiments were approved by the Institutional Animal Care and Use Committee (IACUC) of Shanghai Jiao Tong University.

Consent to publish

Not applicable.

Availability of data and materials

The datasets generated and analyzed during the current study are available from the corresponding author on reasonable request.

Competing interests

The authors declare that they have no competing interests.

Funding

This work was supported in part by the National Natural Science Foundation of China (82002922) and Natural Science Foundation of Shanghai (18ZR1423000). The funding did not affect the design of the study, collection, analysis or interpretation of data or preparation of the manuscript.

Authors' Contributions

ZL performed all of the experiments. HLZ performed the flow cytometric cell cycle analysis and immunoprecipitation assays. SLL performed the immunofluorescence assays and lentiviral transduction. CZ performed the quantitative real-time RT-PCR and RNA interference. QXY and QWZ designed the study, analyzed the data, and wrote the paper. QWZ and FHG were responsible for the project development, data collection, data analysis, and manuscript writing. All authors have read and approved the manuscript.

Acknowledgments

Not applicable.

References

1. Satyanarayana A, Kaldis P: **Mammalian cell-cycle regulation: several Cdks, numerous cyclins and diverse compensatory mechanisms**. *Oncogene* 2009, **28**(33):2925-2939.
2. Hydbring P, Malumbres M, Sicinski P: **Non-canonical functions of cell cycle cyclins and cyclin-dependent kinases**. *Nat Rev Mol Cell Biol* 2016, **17**(5):280-292.
3. Hochegger H, Takeda S, Hunt T: **Cyclin-dependent kinases and cell-cycle transitions: does one fit all?** *Nat Rev Mol Cell Biol* 2008, **9**(11):910-916.
4. Lapenna S, Giordano A: **Cell cycle kinases as therapeutic targets for cancer**. *Nat Rev Drug Discov* 2009, **8**(7):547-566.
5. Malumbres M, Barbacid M: **Cell cycle, CDKs and cancer: a changing paradigm**. *Nat Rev Cancer* 2009, **9**(3):153-166.
6. Fingar DC, Blenis J: **Target of rapamycin (TOR): an integrator of nutrient and growth factor signals and coordinator of cell growth and cell cycle progression**. *Oncogene* 2004, **23**(18):3151-3171.
7. Marathe S, Liu S, Brai E, Kaczarowski M, Alberi L: **Notch signaling in response to excitotoxicity induces neurodegeneration via erroneous cell cycle reentry**. *Cell Death Differ* 2015, **22**(11):1775-1784.
8. Garcia-Echeverria C, Sellers WR: **Drug discovery approaches targeting the PI3K/Akt pathway in cancer**. *Oncogene* 2008, **27**(41):5511-5526.
9. Dancey J: **mTOR signaling and drug development in cancer**. *Nat Rev Clin Oncol* 2010, **7**(4):209-219.

10. Engelman JA: **Targeting PI3K signalling in cancer: opportunities, challenges and limitations**. *Nat Rev Cancer* 2009, **9**(8):550-562.
11. Bhende PM, Park SI, Lim MS, Dittmer DP, Damania B: **The dual PI3K/mTOR inhibitor, NVP-BEZ235, is efficacious against follicular lymphoma**. *Leukemia* 2010, **24**(10):1781-1784.
12. Cao P, Maira SM, Garcia-Echeverria C, Hedley DW: **Activity of a novel, dual PI3-kinase/mTor inhibitor NVP-BEZ235 against primary human pancreatic cancers grown as orthotopic xenografts**. *Br J Cancer* 2009, **100**(8):1267-1276.
13. Zhang LD, Liu Z, Liu H, Ran DM, Guo JH, Jiang B, Wu YL, Gao FH: **Oridonin enhances the anticancer activity of NVP-BEZ235 against neuroblastoma cells in vitro and in vivo through autophagy**. *Int J Oncol* 2016, **49**(2):657-665.
14. Gobin B, Battaglia S, Lanel R, Chesneau J, Amiaud J, Redini F, Ory B, Heymann D: **NVP-BEZ235, a dual PI3K/mTOR inhibitor, inhibits osteosarcoma cell proliferation and tumor development in vivo with an improved survival rate**. *Cancer Lett* 2014, **344**(2):291-298.
15. Jin Z, Qing K, Ouyang Y, Liu Z, Wang W, Li X, Xu Z, Li J: **Low dose of lenalidmide and PI3K/mTOR inhibitor trigger synergistic cytoxicity in activated B cell-like subtype of diffuse large B cell lymphoma**. *J Exp Clin Cancer Res* 2016, **35**:52.
16. Ma BB, Lui VW, Hui CW, Lau CP, Wong CH, Hui EP, Ng MH, Cheng SH, Tsao SW, Tsang CM *et al*: **Preclinical evaluation of the mTOR-PI3K inhibitor BEZ235 in nasopharyngeal cancer models**. *Cancer Lett* 2014, **343**(1):24-32.
17. Chang L, Graham PH, Hao J, Ni J, Bucci J, Cozzi PJ, Kearsley JH, Li Y: **PI3K/Akt/mTOR pathway inhibitors enhance radiosensitivity in radioresistant prostate cancer cells through inducing apoptosis, reducing autophagy, suppressing NHEJ and HR repair pathways**. *Cell Death Dis* 2014, **5**:e1437.
18. Kuger S, Graus D, Brendtke R, Gunther N, Katzer A, Lutyj P, Polat B, Chatterjee M, Sukhorukov VL, Flentje M *et al*: **Radiosensitization of Glioblastoma Cell Lines by the Dual PI3K and mTOR Inhibitor NVP-BEZ235 Depends on Drug-Irradiation Schedule**. *Transl Oncol* 2013, **6**(2):169-179.
19. Liu SL, Liu Z, Zhang LD, Zhu HQ, Guo JH, Zhao M, Wu YL, Liu F, Gao FH: **GSK3beta-dependent cyclin D1 and cyclin E1 degradation is indispensable for NVP-BEZ235 induced G0/G1 arrest in neuroblastoma cells**. *Cell Cycle* 2017, **16**(24):2386-2395.
20. Gladden AB, Diehl JA: **Cell cycle progression without cyclin E/CDK2: breaking down the walls of dogma**. *Cancer Cell* 2003, **4**(3):160-162.
21. Hale AN, Ledbetter DJ, Gawriluk TR, Rucker EB, 3rd: **Autophagy: regulation and role in development**. *Autophagy* 2013, **9**(7):951-972.
22. Johansen T, Lamark T: **Selective autophagy mediated by autophagic adapter proteins**. *Autophagy* 2011, **7**(3):279-296.
23. Olson OC, Joyce JA: **Cysteine cathepsin proteases: regulators of cancer progression and therapeutic response**. *Nat Rev Cancer* 2015, **15**(12):712-729.
24. Fruman DA, Rommel C: **PI3K and cancer: lessons, challenges and opportunities**. *Nat Rev Drug Discov* 2014, **13**(2):140-156.

25. Cebulla J, Huuse EM, Pettersen K, van der Veen A, Kim E, Andersen S, Prestvik WS, Bofin AM, Pathak AP, Bjorkoy G *et al*: **MRI reveals the in vivo cellular and vascular response to BEZ235 in ovarian cancer xenografts with different PI3-kinase pathway activity**. *Br J Cancer* 2015, **112**(3):504-513.
26. Piao J, Chen L, Quan T, Li L, Quan C, Piao Y, Jin T, Lin Z: **Superior efficacy of co-treatment with the dual PI3K/mTOR inhibitor BEZ235 and histone deacetylase inhibitor Trichostatin A against NSCLC**. *Oncotarget* 2016.
27. Shao J, Sheng H, DuBois RN, Beauchamp RD: **Oncogenic Ras-mediated cell growth arrest and apoptosis are associated with increased ubiquitin-dependent cyclin D1 degradation**. *J Biol Chem* 2000, **275**(30):22916-22924.
28. Wang H, Zhang X, Geng L, Teng L, Legerski RJ: **Artemis regulates cell cycle recovery from the S phase checkpoint by promoting degradation of cyclin E**. *J Biol Chem* 2009, **284**(27):18236-18243.
29. Yu XJ, Han QB, Wen ZS, Ma L, Gao J, Zhou GB: **Gambogenic acid induces G1 arrest via GSK3beta-dependent cyclin D1 degradation and triggers autophagy in lung cancer cells**. *Cancer Lett* 2012, **322**(2):185-194.
30. Chen Z, Wang Z, Pang JC, Yu Y, Bieerkehazhi S, Lu J, Hu T, Zhao Y, Xu X, Zhang H *et al*: **Multiple CDK inhibitor dinaciclib suppresses neuroblastoma growth via inhibiting CDK2 and CDK9 activity**. *Sci Rep* 2016, **6**:29090.
31. Xie S, Jiang H, Zhai XW, Wei F, Wang SD, Ding J, Chen Y: **Antitumor action of CDK inhibitor LS-007 as a single agent and in combination with ABT-199 against human acute leukemia cells**. *Acta Pharmacol Sin* 2016.
32. Calvisi DF, Ladu S, Pinna F, Frau M, Tomasi ML, Sini M, Simile MM, Bonelli P, Muroni MR, Seddaiu MA *et al*: **SKP2 and CKS1 promote degradation of cell cycle regulators and are associated with hepatocellular carcinoma prognosis**. *Gastroenterology* 2009, **137**(5):1816-1826 e1811-1810.
33. Meng LH, Zhang H, Hayward L, Takemura H, Shao RG, Pommier Y: **Tetrandrine induces early G1 arrest in human colon carcinoma cells by down-regulating the activity and inducing the degradation of G1-S-specific cyclin-dependent kinases and by inducing p53 and p21Cip1**. *Cancer Res* 2004, **64**(24):9086-9092.
34. Vymetalova L, Krystof V: **Potential Clinical Uses of CDK Inhibitors: Lessons from Synthetic Lethality Screens**. *Med Res Rev* 2015, **35**(6):1156-1174.
35. Herrero-Ruiz J, Mora-Santos M, Giraldez S, Saez C, Japon MA, Tortolero M, Romero F: **betaTrCP controls the lysosome-mediated degradation of CDK1, whose accumulation correlates with tumor malignancy**. *Oncotarget* 2014, **5**(17):7563-7574.
36. Tao GZ, Rott LS, Lowe AW, Omary MB: **Hyposmotic stress induces cell growth arrest via proteasome activation and cyclin/cyclin-dependent kinase degradation**. *J Biol Chem* 2002, **277**(22):19295-19303.
37. Hirano S, Uemura T, Annoh H, Fujita N, Waguri S, Itoh T, Fukuda M: **Differing susceptibility to autophagic degradation of two LC3-binding proteins: SQSTM1/p62 and TBC1D25/OATL1**. *Autophagy* 2016, **12**(2):312-326.

38. Tatti M, Motta M, Di Bartolomeo S, Cianfanelli V, Salvioli R: **Cathepsin-mediated regulation of autophagy in saposin C deficiency**. *Autophagy* 2013, **9**(2):241-243.

39. Zhao X, Fang Y, Yang Y, Qin Y, Wu P, Wang T, Lai H, Meng L, Wang D, Zheng Z *et al*: **Elaiophylin, a novel autophagy inhibitor, exerts antitumor activity as a single agent in ovarian cancer cells**. *Autophagy* 2015, **11**(10):1849-1863.

Figures

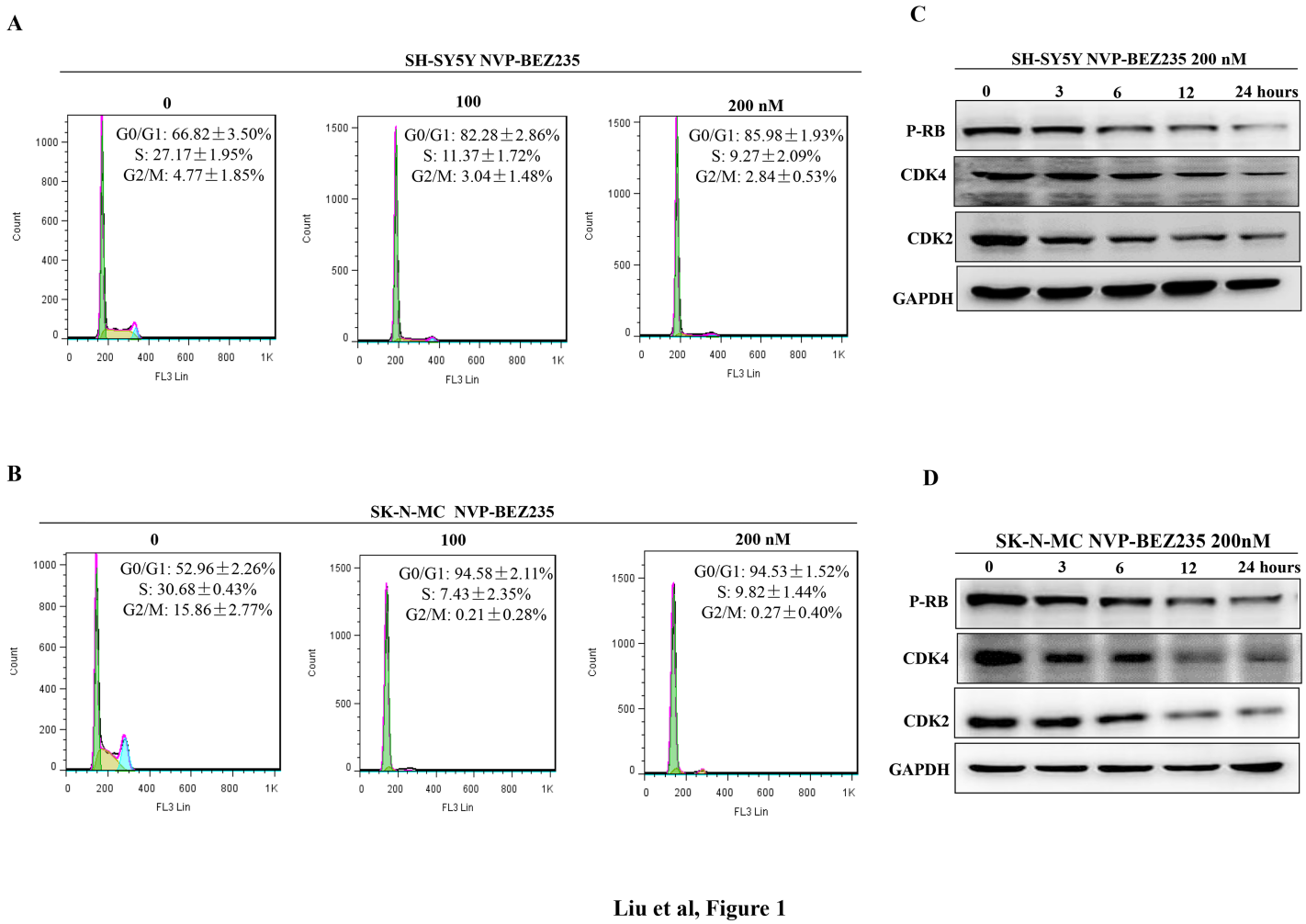

Liu et al, Figure 1

Figure 1

NVP-BEZ235 induced G0/G1 cell cycle arrest with the down regulation of CDK4 and CDK2 in NB cells. (A and B) SH-SY5Y and SK-N-MC cells were treated with NVP-BEZ235 (100, 200 nM) for 24 hours. The cell cycle was assessed by flow cytometry analysis, which determined the cellular DNA content with a hypotonic PI solution. (C and D) SH-SY5Y and SK-N-MC cells were treated with NVP-BEZ235 (200 nM) for the indicated time. Proteins related to the cell cycle were analysed by Western blot analysis (Supplementary figure for Figure 1C and D).

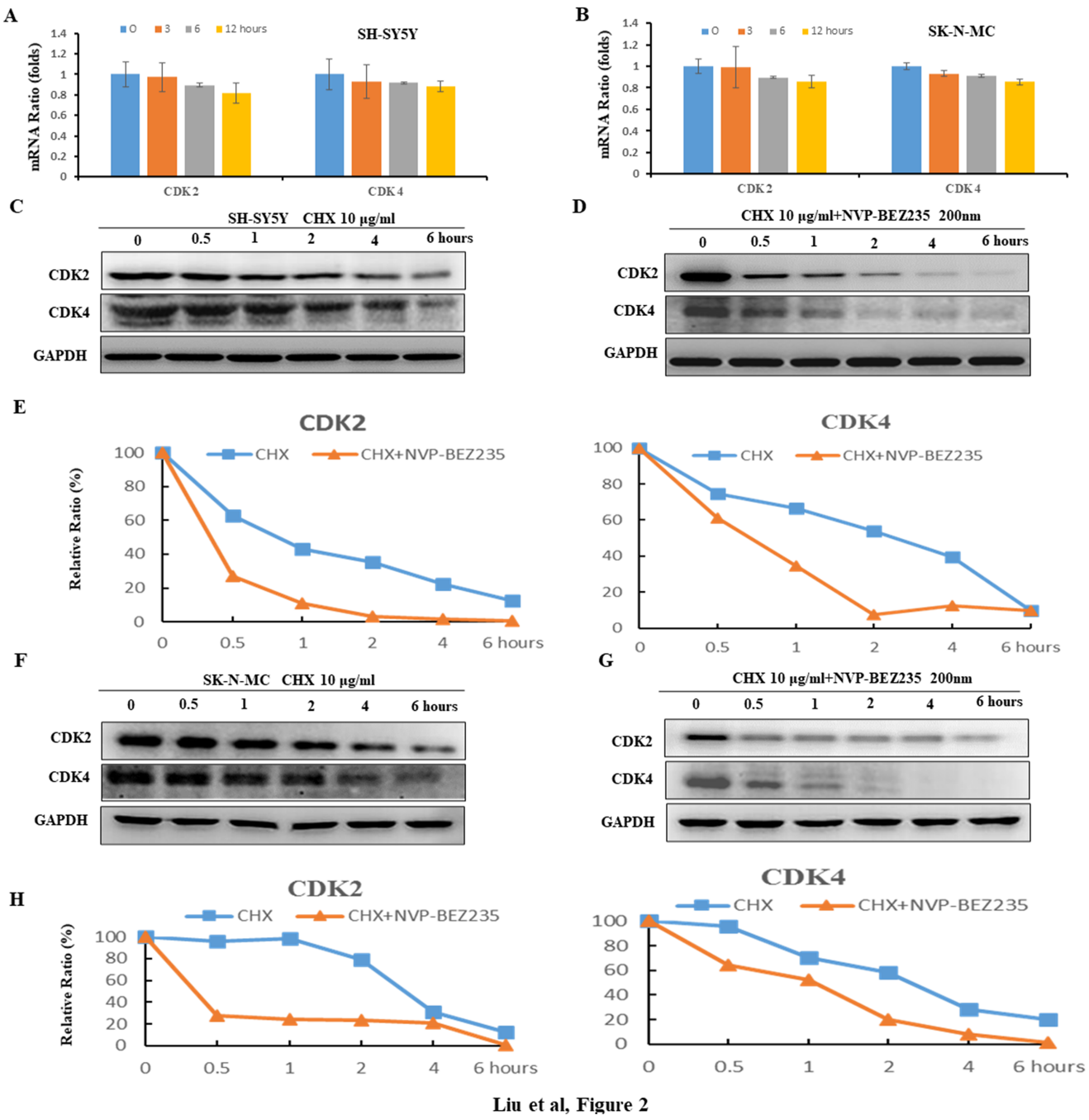

Figure 2

NVP-BEZ235 decreased CDK4 and CDK2 levels by enhancing their protein degradation. (A and B) SH-SY5Y and SK-N-MC cells were incubated with NVP-BEZ235 for the indicated time periods. CDK2 and CDK4 mRNA levels were determined by qRT-PCR. (C, D, E, F, G and H) SH-SY5Y and SK-N-MC cells were pretreated with vehicle or 200 nM NVP-BEZ235 for 1 hour, and then 10 μg/ml CHX was added for various additional time. The respective protein levels were detected by immunoblotting and quantified by densitometry (Supplementary figure for Figure 2-1/2 C, D, F and G).

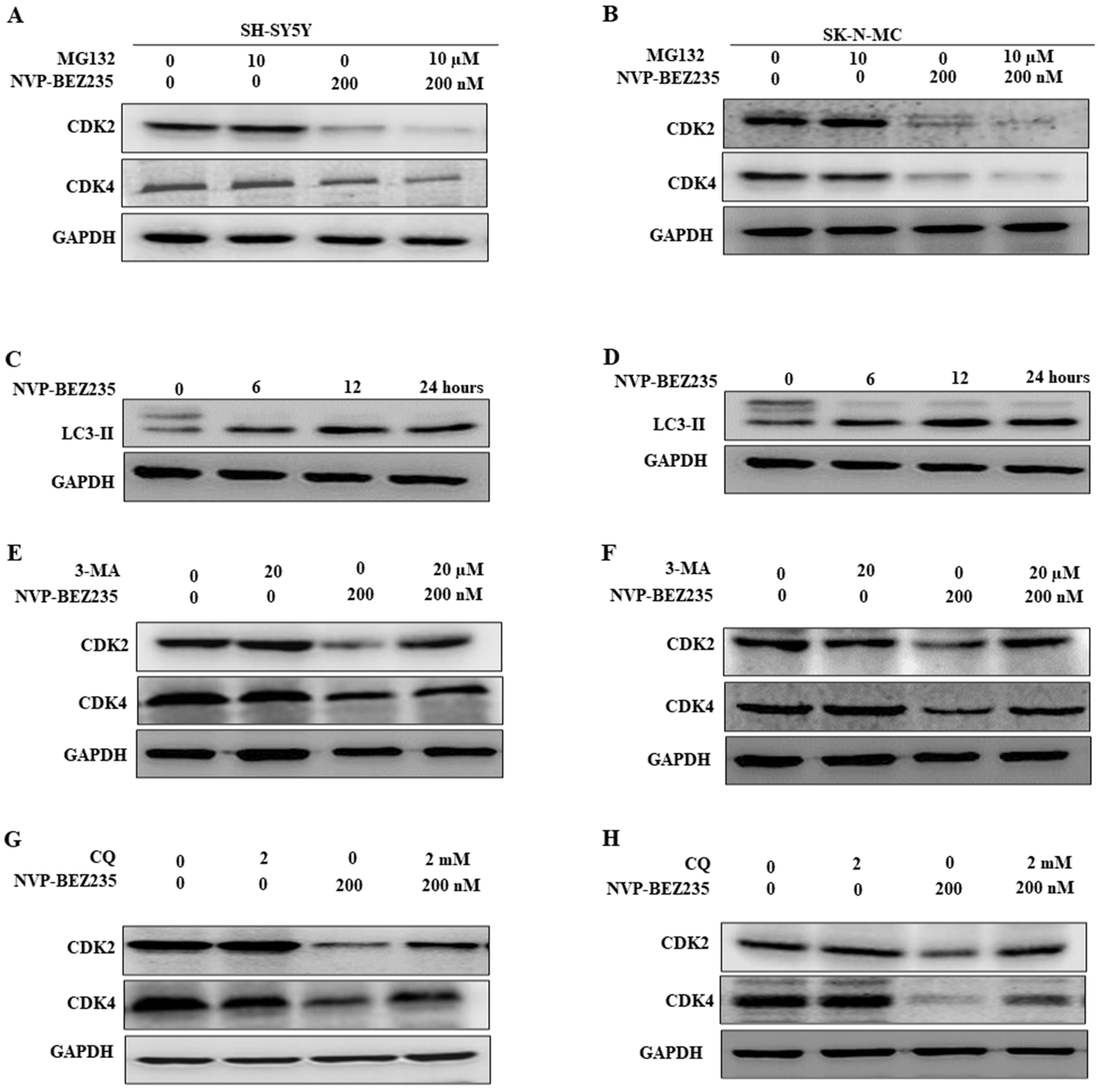

Liu et al, Figure 3

Figure 3

The autophagy-lysosome pathway was involved in NVP-BEZ235-induced degradation of the CDK4 and CDK2 proteins. (A and B) SH-SY5Y and SK-N-MC cells were pretreated for 1 hour with 10 μM proteasome inhibitor (MG132) and subsequently treated for another 12 hours with 200 nM NVP-BEZ235, and the lysates were probed for CDK2 and CDK4 antibodies by immunoblotting (Supplementary figure for Figure 3-1A and B). (C and D) Western blot analysis of the LC3 protein in SH-SY5Y and SK-N-MC cells treated

with 200 nM NVP-BEZ235 for 6, 12 and 24 hours (Supplementary figure for Figure 3-1C and D). (E, F, G and H) SK-N-MC cells were pretreated for 1 hour with an autophagy inhibitor (20 μM CQ or 2 mM 3MA) and subsequently treated for another 12 hours with 200 nM NVP-BEZ235. Western blot analyzed CDK4 and CDK2 proteins (Supplementary figure for Figure 3-2E, F, G and H).

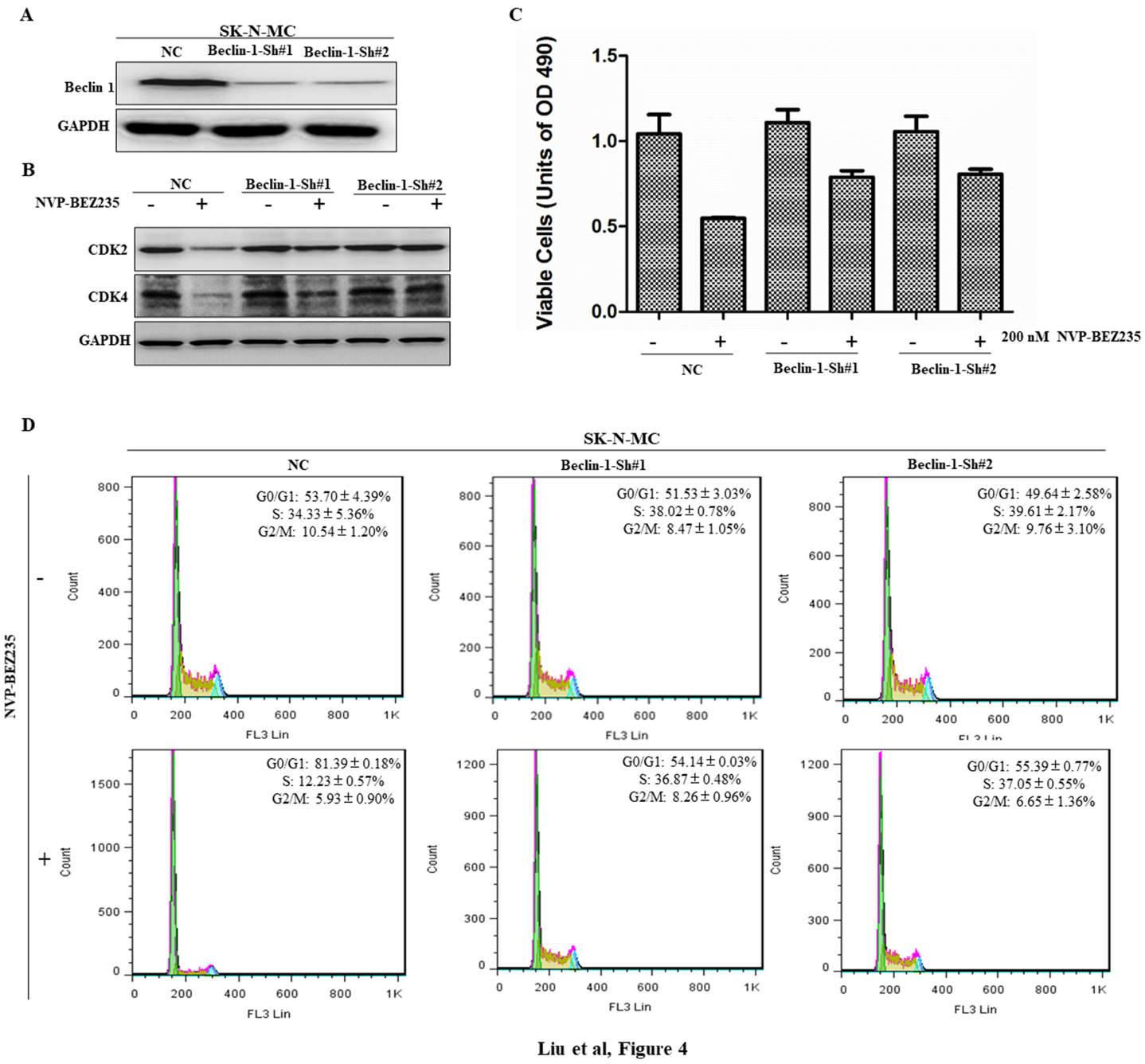

Liu et al, Figure 4

Figure 4

The autophagic degradation pathway was indispensable for NVP-BEZ235-induced CDK4 and CDK2 degradation. (A) SK-N-MC cells were transfected with shRNA specifically targeting Beclin-1 and then assessed by immunoblotting with an anti-Beclin-1 antibody. Transfected cells with individual shRNAs were subsequently treated for 12 hours with vehicle or 200 nM NVP-BEZ235 (Supplementary figure for Figure 4A). (B) The indicated proteins were analysed by immunoblotting (Supplementary figure for Figure

4B). (C) Cell viability was assessed using a CCK-8 assay. (D) Cell cycle distribution is shown by a flow cytometric analysis.

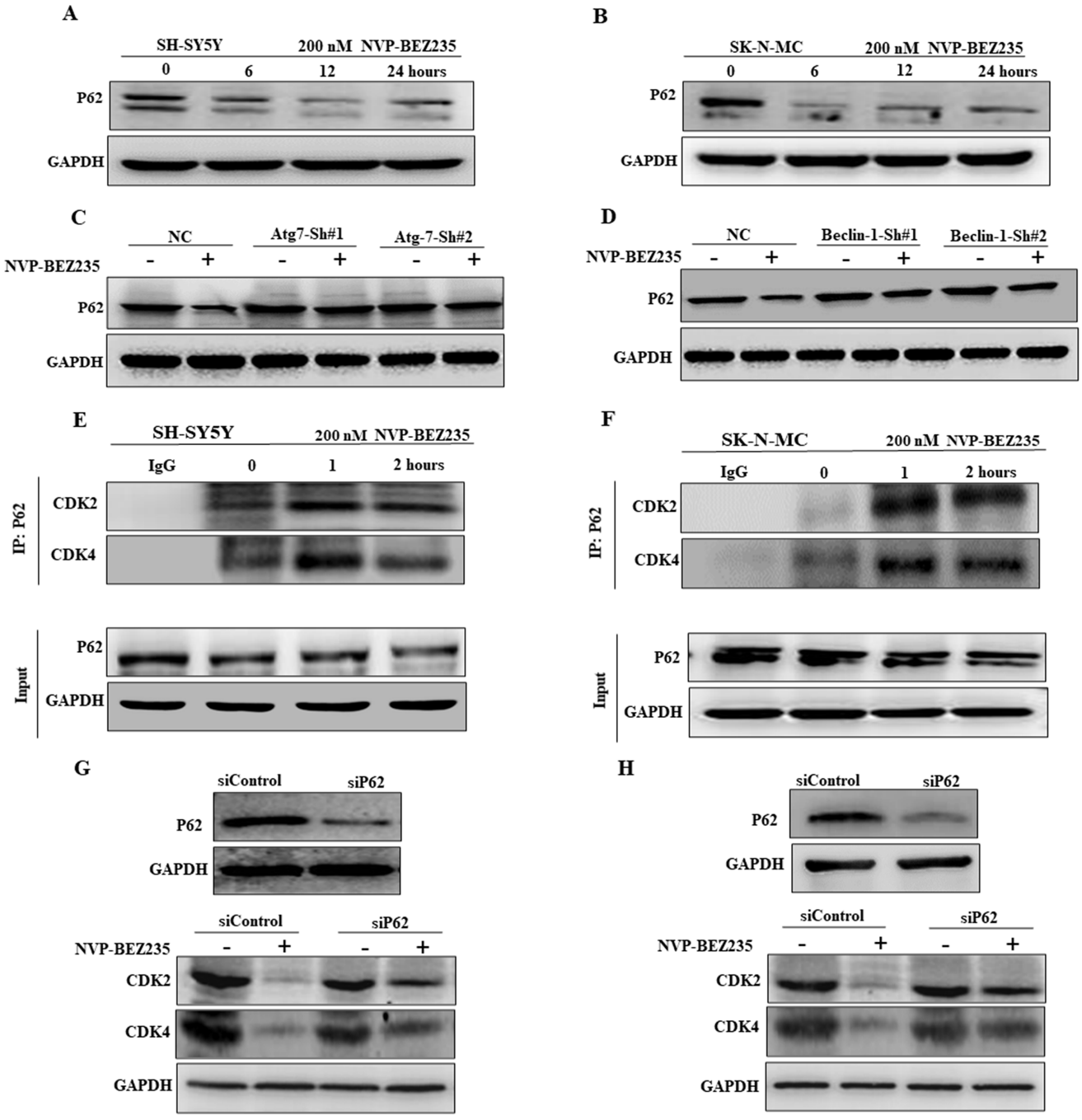

Figure 5

P62 mediated NVP-BEZ235-induced autophagic degradation of the CDK2 and CDK4 proteins. (A and B) SH-SY5Y and SK-N-MC cells were incubated for the indicated times with 200 nM NVP-BEZ235 and then assessed by immunoblotting with an anti-p62 antibody (Supplementary figure for Figure 5-1A and B). (C and D) ATG7-deleted SH-SY5Y cells and Beclin-1-deleted SK-N-MC cells were treated for 12 hours with vehicle or 200 nM NVP-BEZ235 and then lysed and analyzed by immunoblotting with an anti-p62

antibody (Supplementary figure for Figure 5-1C and D). (E and F) After SH-SY5Y and SK-N-MC cells were incubated for the indicated times with 200 nM NVP-BEZ235. Cell lysates were immunoprecipitated with an anti-p62 antibody and then probed with anti-CDK2 and anti-CDK4 antibodies (Supplementary figure for Figure 5-2E and F). (G and H) SH-SY5Y and SK-N-MC cells were transfected with siRNA targeting p62 for 36 hours and then treated with 200 nM NVP-BEZ235 for another 12 hours. The cells were lysed and analyzed by immunoblotting with antibodies against CDK2 and CDK4 (Supplementary figure for Figure 5-2G and H).

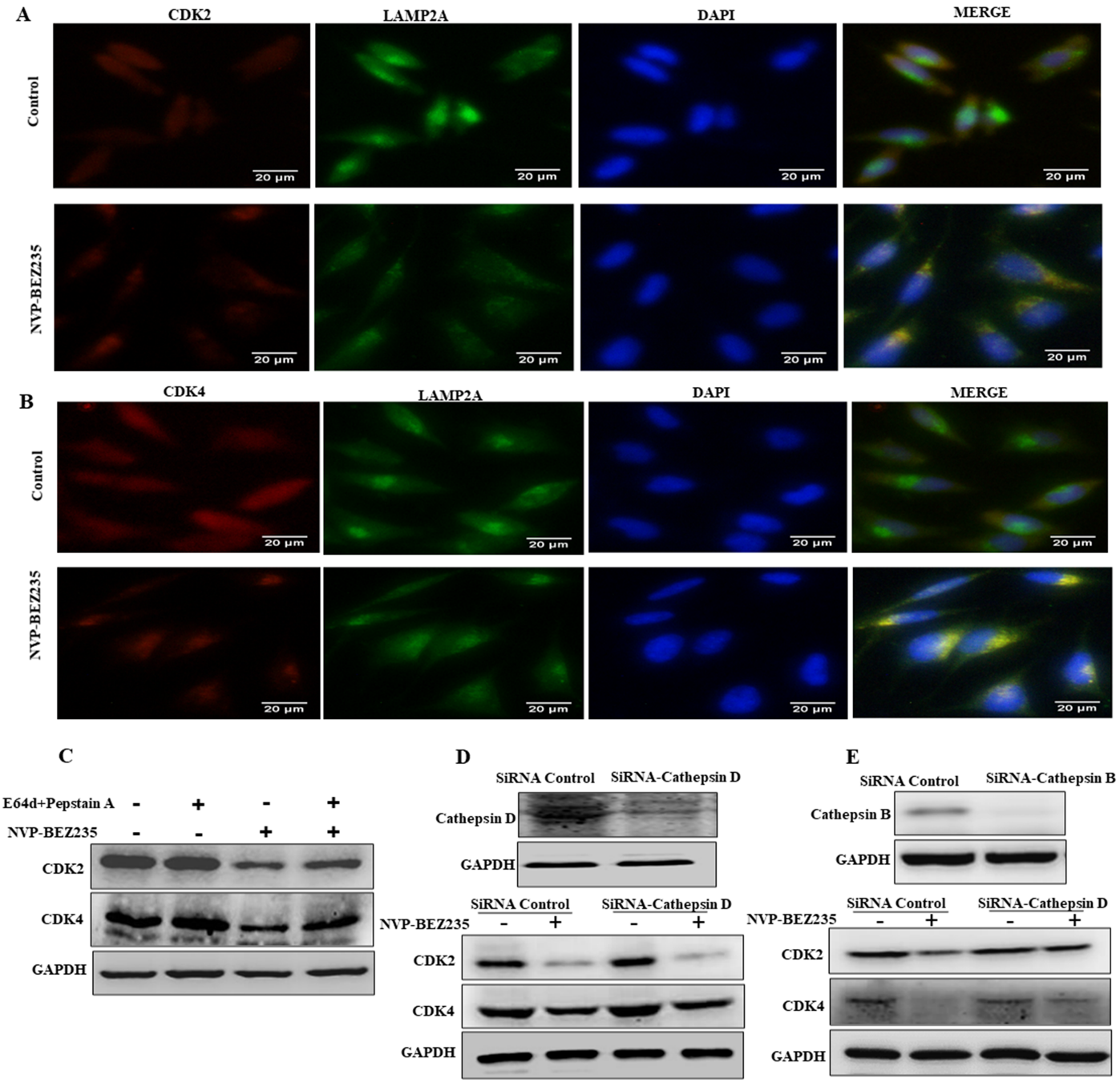

Figure 6

CTSB was required for NVP-BEZ235-induced autophagic degradation of the CDK2 and CDK4 proteins. (A and B) SH-SY5Y cells treated with 200 nM NVP-BEZ235 for 12 hours were stained with anti-LAMP2 (green), anti-CDK2 (red) or anti-CDK4 (red) antibodies, and the signals were detected by fluorescence microscopy. Merged panels indicate the overlapped images of the 2 fluorescent signals. Scale bars: 20 μm. (C) SH-SY5Y cells were pretreated for 1 hour with pepstatin A (10 μM) and E64-d (10 μM) and subsequently treated with 200 nM NVP-BEZ235 for another 12 hours. The cells were lysed and analyzed by immunoblotting with antibodies against CDK2 and CDK4 (Supplementary figure for Figure 6-1C). (D and E). SH-SY5Y cells were transfected with siRNA targeting CTSB or CTSD for 36 hours and then treated with 200 nM NVP-BEZ235 for another 12 hours. The cells were lysed and analyzed by immunoblotting with antibodies against CDK2 and CDK4 (Supplementary figure for Figure 6-1D and Figure 6-2E).

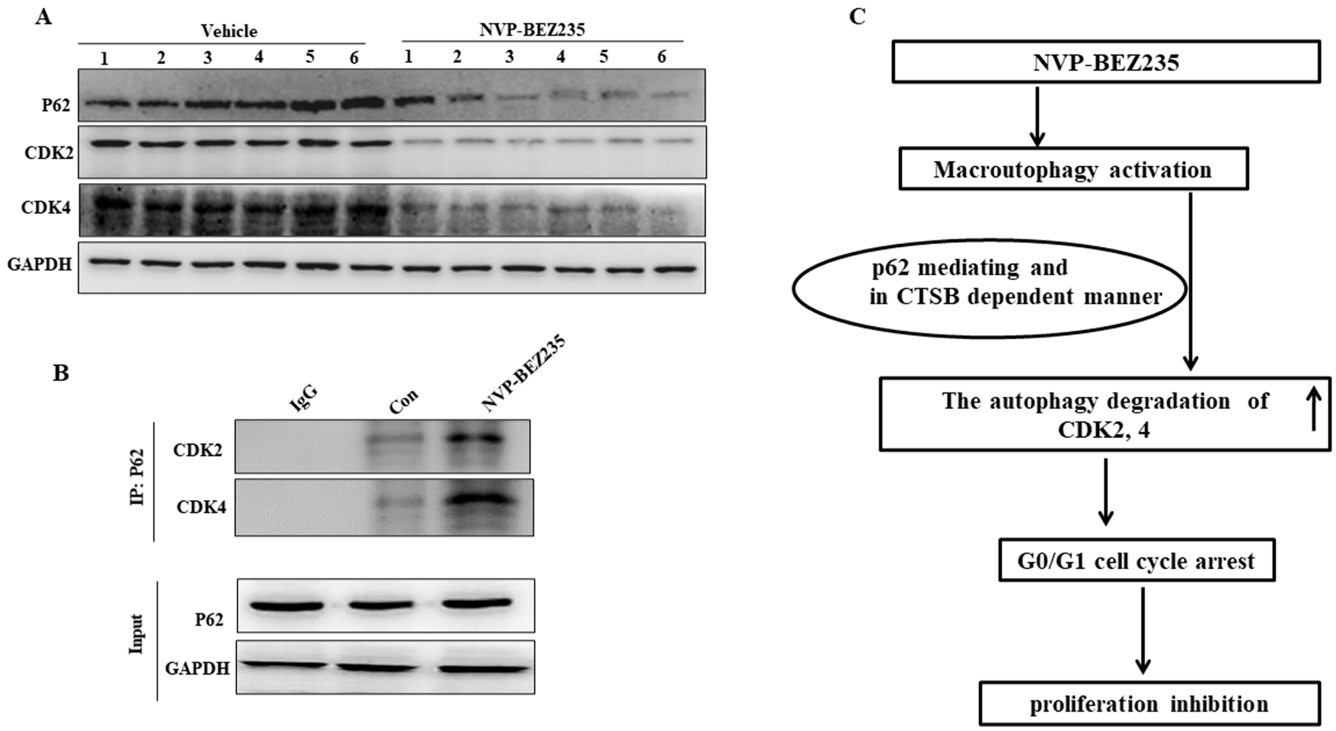

Liu et al, Figure 7

Figure 7

NVP-BEZ235-induced autophagic degradation of the CDK2 and CDK4 proteins in NB xenograft tumors. (A) Tumor extracts were lysed and analyzed by immunoblotting with antibodies against p62, CDK2 and CDK4 proteins (Supplementary figure for Figure 7A). (B) Tumor extracts were immunoprecipitated (IP) with an anti-p62 antibody followed by immunoblotting with anti-CDK2 or CDK4 antibodies (Supplementary figure for Figure 7B). (C) Schematic presentation of the degradation of CDK2 and CDK4. NVP-BEZ235 induces the interaction of p62/SQSMT1 with CDK2 or CDK4 and the subsequent autophagic degradation of CDK2 and CDK4 in a CTSB-dependent manner. In addition, CDK2 and CDK4

protein degradation by autophagic lysosomes contributes to G0/G1 cell-cycle arrest and proliferation inhibition induced by NVP-BEZ235.

Supplementary Files

This is a list of supplementary files associated with this preprint. Click to download.

- SupplementaryfigureforFigure1.tif
- SupplementaryfigureforFigure21.tif
- SupplementaryfigureforFigure22.tif
- SupplementaryfigureforFigure31.tif
- SupplementaryfigureforFigure32.tif
- SupplementaryfigureforFigure4.tif
- SupplementaryfigureforFigure51.tif
- SupplementaryfigureforFigure52.tif
- SupplementaryfigureforFigure61.tif
- SupplementaryfigureforFigure62.tif
- SupplementaryfigureforFigure7.tif